Aberrant Neurofilament Phosphorylation in Sensory Neurons of Rats With Diabetic Neuropathy

Paul Fernyhough, Alex Gallagher, Sharon A. Averill, John V. Priestley, Luke Hounsom, Jyoti Patel, and David R. Tomlinson

Aberrant neurofilament phosphorylation occurs in many neurodegenerative diseases, and in this study, two animal models of type 1 diabetes—the spontaneously diabetic BB rat and the streptozocin-induced diabetic rat—have been used to determine whether such a phenomenon is involved in the etiology of the symmetrical sensory polyneuropathy commonly associated with diabetes. There was a two- to threefold ($P < 0.05$) elevation of neurofilament phosphorylation in lumbar dorsal root ganglia (DRG) of diabetic rats that was localized to perikarya of medium to large neurons using immunocytochemistry. Additionally, diabetes enhanced neurofilament M phosphorylation by 2.5-fold ($P < 0.001$) in sural nerve of BB rats. Neurofilaments are substrates of the mitogen-activated protein kinase (MAPK) family, which includes c-jun NH_2-terminal kinase (JNK) or stress-activated protein kinase (SAPK1) and extracellular signal-regulated kinases (ERKs) 1 and 2. Diabetes induced a significant three- to fourfold ($P < 0.05$) increase in phosphorylation of a 54-kDa isoform of JNK in DRG and sural nerve, and this correlated with elevated c-Jun and neurofilament phosphorylation. In diabetes, ERK phosphorylation was also increased in the DRG, but not in sural nerve. Immunocytochemistry showed that JNK was present in sensory neuron perikarya and axons. Motoneuron perikarya and peroneal nerve of diabetic rats showed no evidence of increased neurofilament phosphorylation and failed to exhibit phosphorylation of JNK. It is hypothesized that in sensory neurons of diabetic rats, aberrant phosphorylation of neurofilament may contribute to the distal sensory axonopathy observed in diabetes. *Diabetes* 48:881–889, 1999

From the Division of Neuroscience (P.F., A.G., L.H., J.P., D.R.T.), School of Biological Sciences, University of Manchester, Manchester; and the Neuroscience Section (S.A.A., J.V.P.), Division of Biomedical Sciences, St. Bartholomew's and The Royal London School of Medicine and Dentistry, Queen Mary and Westfield College, University of London, London, U.K.

Address correspondence and reprint requests to Dr. Paul Fernyhough, Division of Neuroscience, School of Biological Sciences, 1.124 Stopford Building, University of Manchester, Manchester M13 9PT, U.K. E-mail: paul.fernyhough@man.ac.uk.

Received for publication 28 July 1998 and accepted in revised form 17 December 1998.

ANOVA, analysis of variance; CGRP, calcitonin gene-related peptide; CNS, central nervous system; DRG, dorsal root ganglia; ERK, extracellular signal-regulated kinase; GAP, growth-associated protein; IDPN, β,β′-iminodipropionitrile; JNK, c-Jun NH_2-terminal kinase; KSP, Lys-Ser-Pro; MAPK, mitogen-activated protein kinase; NFH, heavy neurofilament; NFM, medium neurofilament; PBS, phosphate-buffered saline; SAPK, stress-activated protein kinase; STZ, streptozocin; TSA, tyramide signal amplification.

Symmetrical sensory polyneuropathy, the most common form of diabetic neuropathy in humans, is associated with a spectrum of structural changes in peripheral nerves that include axonal degeneration, paranodal demyelination, and loss of myelinated fibers; the latter is probably the result of a dying-back of distal axons (1,2). In the streptozocin (STZ)-induced diabetic and BB rat animal models of type 1 diabetes, similar structural abnormalities in peripheral nerves have been observed. In addition, however, loss of axonal caliber associated with axonal shrinkage occurs (2–4). This is not seen in humans but may represent an intermediate stage before overt nerve degeneration. Neurofilament proteins are major constituents of the axonal cylinder, and the levels and phosphorylation status of these proteins is believed to determine axonal caliber (5–7). Studies in diabetic rats show reduced sensory neuron expression of neurofilament (8), reduced axonal transport of neurofilament in motor axons (9), loss of neurofilament in distal nerve (10), and abnormal neurofilament phosphorylation in spinal cord and sciatic nerve (11,12).

Enhanced or aberrant neurofilament phosphorylation, and possibly resulting changes in neurofilament organization, is observed in many neurodegenerative diseases of sensory neurons. These include toxic neuropathies induced by cisplatin (13), acrylamide (14), and β,β′-iminodipropionitrile (IDPN) (15). Aberrant neurofilament phosphorylation may also contribute to diseases of the central nervous system (CNS), including amyotrophic lateral sclerosis (16), Parkinson's disease (17), and Alzheimer's disease (18). An important implication, therefore, is that abnormal neurofilament phosphorylation may underlie the loss of caliber and eventual axonal loss observed in diabetic neuropathy.

Several kinases are known to phosphorylate neurofilament. These include c-Jun NH_2-terminal kinase (JNK) or stress-activated protein kinase (SAPK1), extracellular signal-regulated kinases (ERKs) 1 and 2 (19), glycogen synthase kinase-3α (20), and cyclin-dependent kinase-5 (20–22). JNK is a proline-directed kinase belonging to the mitogen-activated protein kinase (MAPK) family (23,24). Studies, mainly in non-neurons in culture, show that numerous extracellular stress-related signals result in activation of these kinases (23,24). The roles of JNK in the nervous system are relatively unknown, but recent studies show a heterogeneous expression of JNK in the CNS and activation in response to extracellular stress (25,26). In PC12 cells and in cultured embryonic sympathetic neurons undergoing apoptosis, induced by removal of nerve growth factor, the activation of JNK occurs at a point

upstream from commitment to cell death (27,28). Most importantly, in cultured PC12 cells and embryonic sensory neurons, activated JNK is capable of enhanced or aberrant phosphorylation of neurofilament in response to stress (29,30).

In diabetic sensory polyneuropathy, the distal dying-back of axons could be a result of deficient neurofilament synthesis and/or delivery (8–10). This, in turn, may be dependent on optimal levels and patterns of neurofilament phosphorylation within sensory neuron perikarya and axons (11,18). The aim of the present study was to determine whether aberrant neurofilament phosphorylation was present within sensory neuron perikarya and distal nerves of animal models of type 1 diabetes and relate this phenomena to the phosphorylation status of JNK.

RESEARCH DESIGN AND METHODS

Experimental diabetes. Male Wistar rats were made diabetic for 6–12 weeks by a single intraperitoneal injection of STZ (55 mg/kg; Sigma, St. Louis, MO). A group of 8-week diabetic rats received an insulin implant (4 IU · day^{-1} · rat^{-1}; Linplants; Møllegaard Breeding Centre, Skensved, Denmark) for the final 4 weeks (31). The level of glucose in tail vein blood was measured using a glucose oxidase strip–operated reflectance meter (Reflolux II BCL; Boehringer Mannheim, Mannheim, Germany), and it was >27 mmol/l for all STZ-injected rats. At death, plasma glucose levels for all groups of diabetic rats were >20 mmol/l (plasma glucose levels for control rats ranged from 10 to 11 mmol/l). Body weights for age-matched control rats ranged from 450 to 500 g, while all groups of diabetic rats were 300–350 g at study end.

The spontaneously diabetic BB rats, a genetic animal model of type 1 diabetes, were derived from a colony maintained at the Biomedical Research Facility at the University of Southampton. Duration of diabetes ranged from 10 to 12 months, and animals received daily injections of insulin to prevent hyperglycemia-induced fatalities. The glycated hemoglobin (% HbA_1) levels were measured using a Sigma kit (Sigma-Aldrich, Poole, Dorset, U.K.) and gave values of 5.72 ± 0.68% for weight-matched control animals and 7.2 ± 0.94% for the BB rats (n = 5–6, P < 0.02). Such a value for the BB rats was indicative of controlled but long-term hyperglycemia. Body weights for both control and BB rats were in the range of 350–375 g at study end.

Sural sensory nerve conduction velocity. Sural sensory nerve conduction velocity was measured in control rats and rats with STZ-induced diabetes of 12 weeks duration, using a novel method. In principle, this involved stimulation of the sural nerve at two points with recording of compound action potentials from the L_4 dorsal root. Rats were anesthetized with urethane (1.25 g/kg i.p.) and placed on a homeothermic blanket (Harvard Apparatus, Cambridge, U.K.). The core body temperature was monitored by a rectal probe and maintained at 37°C. A dorsal laminectomy exposed the lumbar spinal cord, while the spinal column was clamped rostral and caudal to the laminectomy site. An agar mold was formed around the laminectomy site and filled with paraffin oil to insulate the spinal cord. The dura was removed and the left dorsal root S1 cut at a position close to its entry into the spinal cord. The severed dorsal root was then placed over a pair of platinum wire electrodes for the recording of dorsal root volleys. Surgery was also performed on the left hindlimb to expose the sural nerve. The nerve was freed from the surrounding connective tissue, and a pair of platinum wire–stimulating cathodes, fused into a Perspex holder to maintain 8 mm separation, were placed under the nerve. A stainless steel needle electrode was inserted into the surrounding muscle to act as an anode for electrical stimulation. The nerve was continually soaked with paraffin oil to prevent it from drying and was maintained at 37°C. Electrical stimulation (constant current square wave pulses of 0.5 ms duration) was applied to the sural nerve, at a frequency of 1Hz, via the proximal and distal stimulating electrode in turn. The stimulus intensity was set at 1.5 times that of the threshold stimulus current. Recordings made from the dorsal root were amplified 10,000 times (AC preamplifier; Neurolog, Digitimer, Welwyn Garden City, U.K.), filtered, digitized (1401 plus A–D converter; Cambridge Electronic Design, Cambridge, U.K.), and captured using CED Signal Averager software on a PC. Sural nerve conduction velocities were determined from latency differences derived from 8 mm cathodal separation.

Measurement of protein levels using Western blotting. The L_4 and L_5 dorsal root ganglia (DRG) (dorsal roots 1 cm adjacent to ganglion) and 2 cm distal segments of peroneal and sural nerve were taken and frozen in liquid nitrogen and homogenized (32). Briefly, samples were homogenized using a Polytron (Kinematica, Luzerne, Switzerland) in 0.1 mmol/l PIPES (pH 6.9), 5.0 mmol/l $MgCl_2$, 5.0 mmol/l EGTA, 0.5% Triton X-100, 20% glycerol, 1.0 mmol/l phenylmethylsulfonyl fluoride, and a mixture of protease inhibitors (1.0 µg/ml pepstatin A, 1.0 µg/ml leupeptin, 10 µg/ml benzoyl-L-arginine methyl ester, 10 µg/ml p-tosyl-L-arginine methyl ester, 10 µg/ml soybean trypsin inhibitor, 10 µg/ml L-1-tosylamide-2 phenylethylchloromethyl ketone, and 7 µg/ml aprotinin). SDS-PAGE (8% acrylamide) was performed on 10 µg of protein, and the separated proteins were transferred to nitrocellulose (Amersham ECL [enhanced chemiluminescence] membrane, Amersham, U.K.) using a graphite blotter. Primary antibodies used were SMI-31 (1:50,000 dilution), anti-phosphorylated heavy neurofilament (NFH) (~210 kDa) and medium neurofilament (NFM) (~160–170 kDa) (33) (Affinity Research, Nottingham, Nottinghamshire, U.K.); SMI-32 (1:5,000), anti-nonphosphorylated NFH/NFM (~200- to 210-kDa and ~160-kDa species, respectively) (33) (Affinity Research); antibodies to total (code FL; 1:1,000) and phosphospecific (code G-7; 1:200; phosphorylated on Thr-183 and Tyr-185) JNK 1 and 2 (Santa Cruz Biotechnology, Santa Cruz, CA); antibodies to total and phosphospecific (phosphorylated on Thr-202/Tyr-204) ERK 1 and 2 (New England Biolabs, Beverley, MA); and antibody to phosphospecific c-Jun (phosphorylated on Ser-63; 1:1,000; Santa Cruz Biotechnology). Detection was achieved using the New England Biolabs phototope-HRP system (Beverley, MA). The relative levels of protein were determined using an image analyzer (AI, Cambridge, U.K.).

Immunocytochemistry for neurofilament and JNK in lumbar DRG, ventral horn, and sciatic nerve. Three control and three 12-week STZ-induced diabetic rats were used for immunocytochemical analysis using standard techniques (34). Animals were anesthetized with sodium pentobarbital (60 mg/kg) and perfused through the ascending aorta with saline, followed by 300 ml of 4% paraformaldehyde in 0.1 mol/l phosphate buffer, pH 7.4. The L_4 and L_5 DRG, midsciatic nerve, and ventral horn (at L1) were removed, postfixed for 2 h in the same fixative, and cryoprotected in 15% sucrose overnight. Tissues were frozen and sectioned at 8 µm. Sections were stained using indirect immunofluorescence histochemistry with antibodies directed against total JNK 1 and 2 (code FL) (Santa Cruz Biotechnology) diluted 1:100; phosphospecific JNK diluted 1:100 (dually phosphorylated on Thr-183 and Tyr-185; Promega, Madison, WI); and phosphorylated neurofilament using monoclonal antiseras SMI-31 at 1:100 and RMO-24 at 1:50 (35) (Zymed, San Francisco, CA). Synaptophysin was detected using a rabbit polyclonal diluted at 1:2,000 (Biometra, Gottingen, Germany). Calcitonin gene-related peptide (CGRP) was detected using a rabbit polyclonal at 1:4,000 (36). For detection of primary polyclonal antibody, a donkey anti-rabbit tetramethyl rhodamine isothiocyanate–conjugated secondary antiserum (1:200; Jackson Immunoresearch, West Grove, PA) was used; for detection of monoclonal antibody, a donkey anti-mouse Cy2 conjugate was used (Jackson Immunoresearch). Double labeling of JNK together with synaptophysin, and neurofilament together with CGRP, was achieved using standard indirect immunofluorescence or the tyramide signal amplification (TSA) (Du Pont-NEN, Wilmington, DE) fluorescence technique (34,36). The two sets of antisera were applied sequentially and TSA, if used, was applied to the first series. Control rats showed no artefactual double labeling. After final washes in phosphate-buffered saline (PBS), sections were coverslipped in a PBS/glycerol solution (1:3) containing 2.5% 1,4 diazobicyclo (2,2,2) octane (antifading agent; Sigma). Immunoreactivity was visualized on a Leica epifluorescence microscope using the Y3 and L4 filter block.

Data analysis. Where appropriate, data were subjected to one-way analysis of variance (ANOVA) using the Statistical Package for Social Scientists (SPSS/PC+; SPSS, Chicago). Where the F ratio gave P < 0.05, comparisons between individual group means were made by Duncan's multiple range test at significance levels of P = 0.05 and 0.01. Levene's test was used to examine the data for homogeneity of variance, accepting P > 0.05. Single comparisons between groups were made using a Student's t test. Regression analysis was performed using Excel 5.0 (Microsoft).

RESULTS

Sural sensory nerve conduction velocity. There was a marked slowing of conduction velocity in the sural nerve. Mean values (± 1 SD) were 65.8 ± 12.0 m/s for control rats and 32.3 ± 8.5 m/s for 12-week STZ-induced diabetic rats (P < 0.001).

Diabetes-induced aberrant neurofilament phosphorylation in lumbar DRG. Lumbar DRG homogenates were probed using antibodies specific for nonphosphorylated and phosphorylated neurofilament. Figure 1*B* and Table 1 show that nonphosphorylated NFH levels (detected using antisera SMI-32) did not change between age-matched and 12-week STZ-induced diabetic rats. However, the levels of the phosphorylated NFH and NFM epitopes detected using the SMI-31 antisera were significantly enhanced at 12 weeks of diabetes (P < 0.05 by one-way ANOVA) and reversed by

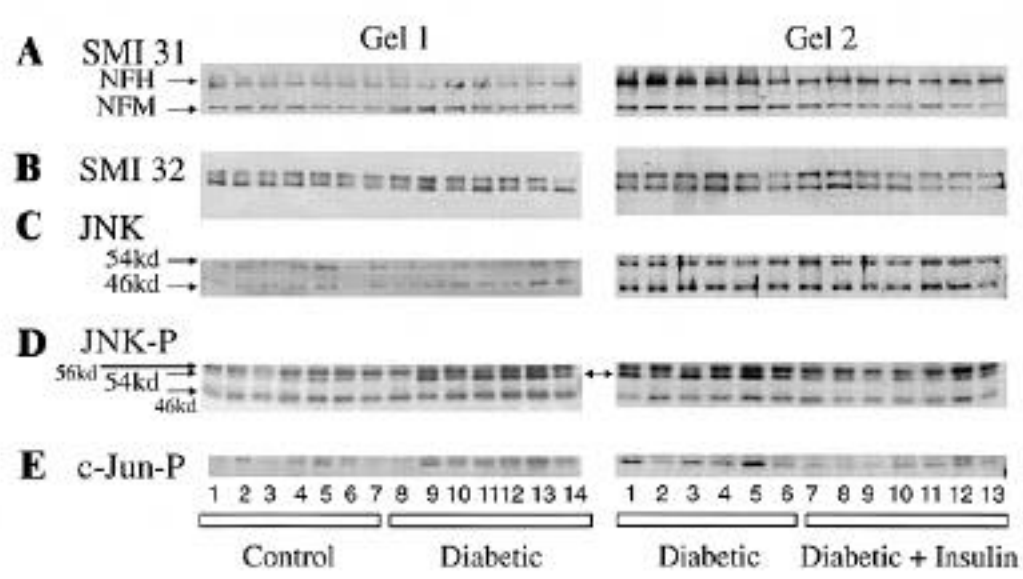

FIG. 1. Western blots for neurofilament and JNK in DRG in STZ-induced diabetic rats. Lumbar DRG homogenates were subjected to Western blotting and probed with a range of antibodies. *A*: SMI-31 antisera detects phosphorylated epitopes of NFH and NFM. *B*: SMI-32 antisera detects nonphosphorylated epitopes of NFH and NFM. *C*: JNK antisera detects all isoforms of JNK 1 and 2. *D*: JNK-P antisera detects activated, i.e., phosphorylated, JNK 1, 2, and 3 α2 and β2 isoforms (37) and shows elevation of 54-kDa isoform in diabetic rats. *E*: c-Jun-P antisera detects phosphorylated c-Jun. Animals were made diabetic for 12 weeks, and insulin therapy was provided for the final 4 weeks for a subgroup. *Gel 1 lanes 1–7*, control; *Gel 1 lanes 8–14*, diabetic. *Gel 2 lanes 1–6*, diabetic (same group as in Gel 1 minus one sample); *Gel 2 lanes 7–13*, diabetic plus insulin.

insulin treatment. There was no elevation of NFM or NFH phosphorylation at 6 weeks of diabetes.

Analysis of tissue homogenates of lumbar dorsal root, taken directly adjacent to the ganglion, from age-matched control and 12-week STZ-induced diabetic rats showed no significant effect of diabetes on NFH or NFM phosphorylation as detected using the SMI-31 antisera (Table 2).

Immunocytochemistry for phosphorylated neurofilament in sensory and motoneurons. Figure 2*A–E* shows immunocytochemistry for phosphorylated NFH and NFM using the SMI-31 and RMO-24 antisera in lumbar DRG from control and 12-week STZ-induced diabetic rats. In DRG of control and diabetic rats, the staining was localized to medium to large perikarya, confirming that highly phosphorylated neurofilament was restricted to myelinated sensory neurons of medium to large caliber (35). Figure 2*B* and *D* shows that diabetes clearly raised the level of staining detected using the SMI-31 and RMO-24 antibodies in medium to large perikarya. Perikarya of small neurons, presumably nociceptive in phenotype, were identified using an antibody to the neuropeptide CGRP. Double labeling using SMI-31 and CGRP antisera revealed that these small neurons continued to show low levels of neurofilament immunoreactivity in diabetic rats (Fig. 2*E* and *F*). Figure 3*A* and *B* shows that aberrant neurofilament phosphorylation detected using antiserum RMO-24 was not induced by 12 weeks' duration of diabetes in lumbar motoneuron perikarya, and similar results were observed using the SMI-31 antisera.

Effect of diabetes on phosphorylation of JNK and ERK in DRG and sural nerve of STZ-induced diabetic rats. Lumbar DRG from age-matched and 12-week STZ-induced diabetic rats were analyzed for JNK and ERK phosphorylation using Western blotting. Figure 1*D* shows that the phospho-specific antibody for JNK, which detects activated (phosphorylated on Thr-183 and Tyr-185) JNK isoforms, detected three activated species, the 54-kDa species being significantly enhanced in diabetic rats. According to the terminology of Gupta et al. (37), this protein species is composed of isoforms of JNK 1, 2, and 3 α2/β2. The ERK antibodies detected ERK species of 44 kDa (ERK 1) and 42 kDa (ERK 2) in all tissues studied (not shown). The levels of total JNK and ERK (nonphosphorylated and phosphorylated) did not differ between treatment groups (Fig. 1*C* and Table 3). Table 3 shows that diabetes significantly enhanced phosphorylation of JNK (54-kDa species) and ERK 2 (ERK 1 and ERK 2 were similarly affected) by four- and fivefold ($P < 0.05$ by one-way ANOVA or Student's t test) in DRG, respectively. For JNK, this effect was significantly attenuated by insulin therapy. Phosphorylated JNK could not be detected in homogenates of lumbar dorsal root of normal or diabetic rats (Table 2). Diabetes of 12

TABLE 1
Effect of STZ-induced diabetes on neurofilament levels and phosphorylation in lumbar DRG

	NFM-P (SMI-31)	NFH-P (SMI-31)	NFH-NP (SMI-32)
Control rats	1.0 ± 0.38*	1.0 ± 0.63*	1.0 ± 0.56
Diabetic rats	2.9 ± 0.25†§	1.9 ± 0.34†	1.13 ± 0.55
Diabetic rats + insulin	2.0 ± 0.56†‡	1.23 ± 0.12*	0.85 ± 0.37

Data are means ± SD (n = 7). DRG homogenates from age-matched control and 12-week STZ-induced diabetic rats were subjected to Western blotting and then probed with monoclonal antibodies SMI-31 and SMI-32. Insulin therapy was applied for the final 4 weeks of the 12 weeks' duration of diabetes. NFH-P and NFM-P, phosphorylated NFH and NFM; NFH-NP, nonphosphorylated NFH. * vs. † and ‡ vs. §, $P < 0.05$ (by one-way ANOVA) within each column.

TABLE 2
Effect of STZ-induced diabetes on neurofilament and JNK phosphorylation in lumbar dorsal root

	NFM-P (SMI-31)	NFH-P (SMI-31)	NFH-NP (SMI-32)	p54 JNK-P
Control rats	1.0 ± 0.21	1.0 ± 0.21	1.0 ± 0.19	ND
Diabetic rats	1.26 ± 0.31	1.27 ± 0.3	1.07 ± 0.1	ND

Data are means ± SD (n = 7). Lumbar L_4 and L_5 dorsal roots from age-matched and 12-week STZ-induced diabetic rats were subjected to Western blotting and probed using antisera SMI-31, SMI-32, and anti-phospho-JNK. ND, below detection limit. No significant differences between any groups.

weeks' duration also significantly elevated phosphorylation of the transcription factor, c-Jun, a substrate for activated JNK (24) (Fig. 1*E* and Table 3). Regression analysis showed that the diabetes-induced phosphorylation of NFM, detected using antisera SMI-31, correlated significantly with the phosphorylation of JNK (r^2 = 0.54; F < 0.002). The phosphorylation of JNK and phosphorylation of c-Jun were also significantly correlated (r^2 = 0.78; F < 0.0002). At 6 weeks of diabetes, there was a twofold elevation of phosphorylation of JNK ($P < 0.05$) but no change in c-Jun phosphorylation (data not shown).

In sural nerve, a 12-week duration of STZ-induced diabetes caused a threefold elevation of phosphorylation of JNK (54-kDa species) while leaving ERK 2 phosphorylation unchanged (Table 3) (ERK 1 was similarly unchanged). The activated form of the related stress-activated kinase, p38 (or HOG1 or SAPK2), could not be detected in DRG or sural nerve homogenates from normal or diabetic rats.

Immunocytochemistry for JNK in sensory and motoneurons. Lumbar DRG from age-matched control and 12-week STZ-induced diabetic rats were stained for total and phospho-JNK. Such staining was qualitatively similar for control and diabetic samples—the control tissue sections are presented. Figure 4*A* and *B* show sensory neurons stained positively using antisera to total and phospho-JNK. Immunoreactivity was present in both cytoplasm and nuclei, but with the total JNK antiserum giving more prominent

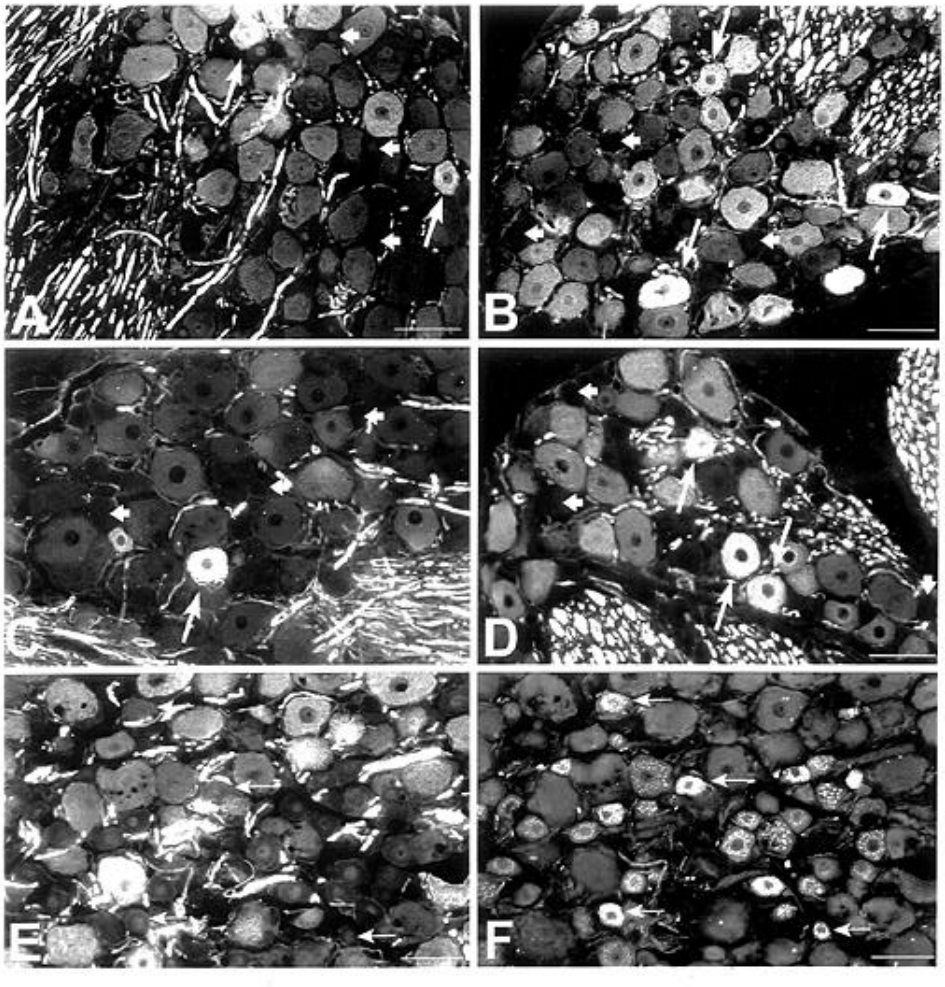

FIG. 2. Immunocytochemistry for phosphorylated neurofilament in lumbar DRG of normal and 12-week STZ-induced diabetic rats. Neurofilament immunoreactivity is greatly increased in large and medium cells of diabetic rats. DRG were stained as follows: control, antiserum SMI-31 (*A*); diabetic, SMI-31 (*B*); control, antiserum RMO-24 (*C*); and diabetic, RMO-24 (*D*). Tissue sections from diabetic rats were also double-labeled using SMI-31 (*E*) and CGRP (*F*). In *A–D*, the arrows indicate highly labeled cells, and the arrowhead shows unlabeled cells. In *E* and *F*, small CGRP immunoreactive cells (arrows) are seen to lack immunoreactivity for phosphorylated neurofilament. Scale bars = 50 μm.

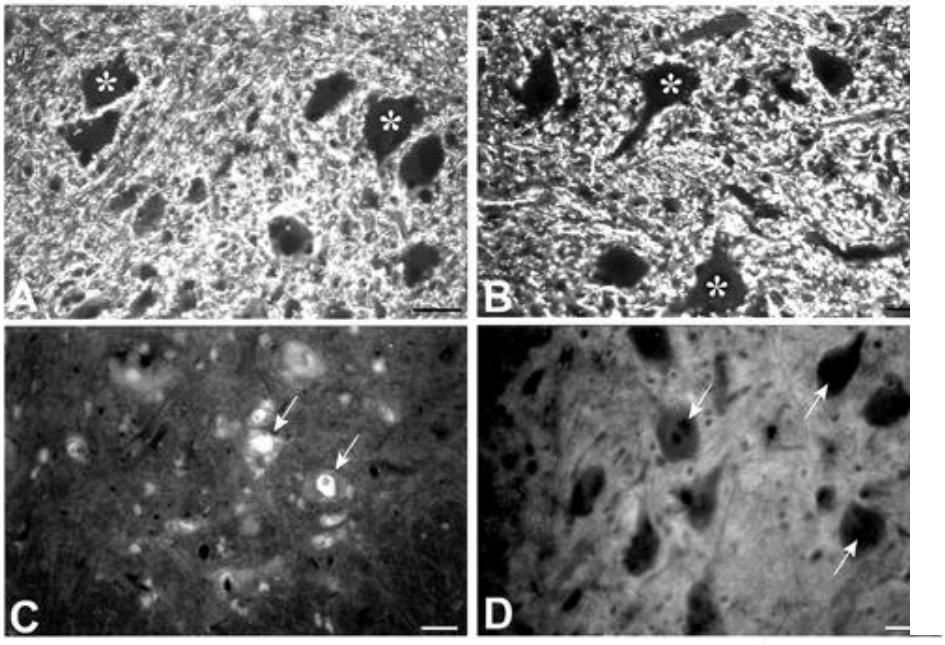

FIG. 3. Immunocytochemistry for neurofilament and JNK in ventral horn. Ventral horn at the L1 level was probed with antiserum RMO-24 in control rats (*A*) and 12-week STZ-induced diabetic rats (*B*). Neurofilament immunoreactivity is weak in motoneurons (asterisks) and is not changed in diabetic rats. Control tissue is stained for total JNK (*C*) and phospho-JNK (*D*). In *C*, arrows show motoneurons stained positively, with nuclear staining paramount. In *D*, there was no staining of motoneurons for phospho-JNK (arrows). Scale bars = 50 μm.

nuclear staining. Most neuronal cells within the ganglia appeared to be positively stained for total and phospho-JNK, but with variations in the level of immunoreactivity. In the ventral horn, motoneuron perikarya stained positively for total JNK. However, motoneuron staining for phospho-JNK was weak compared with surrounding neuropil staining (Fig. 3*C* and *D*). Staining of midsciatic nerve for phospho-JNK (Fig. 4*E* and *F*) revealed a high level of colocalization with synaptophysin, providing evidence of an axonal origin, with little nonaxonal staining. Total JNK staining also colocalized with synaptophysin, suggesting a presence in axons. However, there was also staining in Schwann cells (Fig. 4*C* and *D*).

Aberrant neurofilament phosphorylation and phosphorylation of JNK in DRG of BB rats. Neurofilament phosphorylation and JNK phosphorylation was also studied in the alternative animal model of Type I diabetes, the BB rat. Lumbar DRG homogenates from weight-matched control rats and from BB rats of 10–12 month duration of diabetes were analyzed. Table 4 shows that phosphorylated JNK, the 54-kDa species, was elevated twofold in BB rats ($P < 0.02$) and this correlated with enhanced NFM phosphorylation ($r^2 = 0.67$; $F < 0.002$).

Aberrant neurofilament phosphorylation and phosphorylation of JNK in sural and peroneal nerves of BB rats. The level of NFM phosphorylation was significantly increased by 2.5-fold, and the ratio of phosphorylated NFM to nonphosphorylated NFM rose to 5.43-fold in sural nerve of BB rats (Table 5). There was no significant change in NFM phosphorylation in peroneal nerve. The ratio of phosphorylated NFH to nonphosphorylated NFH was decreased

TABLE 3
Effect of STZ-induced diabetes on ERK, JNK, and c-Jun phosphorylation in lumbar DRG and sural nerve

	n	ERK 2-P (P/Total)	p54 JNK-P (P/Total)	c-Jun-P
DRG				
Control rats	7	1.0 ± 0.38‖	1.0 ± 0.3*	1.0 ± 0.34*
Diabetic rats	6	5.7 ± 0.79‖	4.39 ± 1.71†,§	3.0 ± 0.74†
Diabetic rats + insulin	7	ND	2.39 ± 0.65†,‡	1.23 ± 0.39*
Sural nerve				
Control rats	7	1.0 ± 0.59	1.0 ± 0.32‖	ND
Diabetic rats	7	0.73 ± 0.41	3.04 ± 1.39‖	ND

Data are means ± SD ($n = 4$ for ERK data). Lumbar L_4 and L_5 DRG and sural nerve homogenates from age-matched control and 12-week STZ-induced diabetic rats were subjected to Western blotting and probed for phosphorylated ERK 2 (42-kDa species) and JNK (inclusive of JNK 1, 2, and 3 isoforms α2 and β2; 54-kDa species). Detection was accomplished using antibodies specific for the phosphorylated forms of the kinases. The levels of the phosphorylated JNK species at 56- and 46-kDa were unchanged between control and diabetic groups. The levels of phosphorylated ERK 1 (44-kDa species) were similarly raised in DRG of STZ-induced diabetic rats and were also not altered in sural nerve. The levels of total ERK 2 and JNK did not differ between control and diabetic rats (using polyclonal antisera specific for all ERK and JNK isoforms). c-Jun was detected using an antibody specific for phosphorylated c-Jun. For ERK 2-P and JNK-P, values have been adjusted for total ERK 2 and JNK levels, expressed as P/Total, and then normalized to control. * vs. † and ‡ vs. §, $P < 0.05$ (by one-way ANOVA) within each column; ‖$P < 0.05$ (by Student's t test) for control vs. diabetic rats. Regression analysis: JNK-P vs. c-jun-P; $r^2 = 0.78$ ($F < 0.0002$, highly significant). ND, not determined.

by ~50% in both sural and peroneal nerves of BB rats; this was the result of increased levels of nonphosphorylated NFH. The data in Table 5 show that JNK phosphorylation was elevated 2.88-fold in intact sural (sensory) nerve of BB rats, but there was no significant elevation of phosphorylation of JNK in peroneal (motor) nerve.

DISCUSSION

This study shows that in animal models of type 1 diabetes there is aberrant neurofilament phosphorylation and phosphorylation of the stress-related kinase, JNK, in perikarya and axons of sensory neurons. These observations are important because they provide a fresh framework for the etiology of the symmetrical sensory polyneuropathy commonly associated with diabetes in humans. A major component of the pathology of diabetic neuropathy is the occurrence of a dying-back type of neurodegeneration of distal nerve endings (1,2), resulting in sensory loss and subsequent serious complications for the peripheral tissues (38,39). The Diabetes Control and Complications Trial (40) implicates elevated glucose as a primary metabolic signal for neuropathy. Secondary biochemical transducers may be polyol pathway intermediates (41,42), oxidative stress (43), glycation of proteins (44), or impaired neurotrophic support (45,46). The study presented here provides another biochemical transducer and a target for drug therapy, namely, aberrant neurofilament phosphorylation in sensory neurons, which may be mediated via phosphorylation of JNK. This may, of course, be related to any of the phenomena referred to above, or it may represent a new link between hyperglycemia and nerve damage.

In cisplatin- (13), IDPN- (15) and acrylamide-induced (14) sensory neuropathies and in CNS disease (16,18), aberrant neurofilament phosphorylation has been recognized as an important indicator of neurodegeneration. Aberrant phosphorylation of neurofilament can be defined as the occurrence of phosphorylation at improper levels or sites on neurofilament—usually at serine residues within Lys-Ser-Pro (KSP) motifs of the COOH-terminal tail domain of NFM and NFH (18–20). The important feature of the aberrant phosphorylation observed in these animal models of diabetic neuropathy is its presence in mainly medium to large sensory neurons and absence in small sensory neurons (i.e., low levels of colocalization with CGRP, a marker for small neurons) (Fig. 2*E–F*) and motoneurons. Peripheral axotomy induces aberrant neurofilament phosphorylation within perikarya of medium to large sensory neurons (47–49), with motoneuron perikarya remaining unaffected (47,49). Many changes in gene expression within the DRG of diabetic rats mimic those observed upon axotomy. For example, mRNA levels for γ-preprotachykinin, CGRP, and neurofilament are similarly reduced (5,8,45,46,50), whereas brain-derived neurotrophic factor mRNA levels are elevated (51,52). The changes in expression of growth-associated protein (GAP-43) mRNA do not fit this picture, with diabetes inducing a decrease in expression (8)—the opposite of the change after axotomy (53). A general conclusion is that some aspects of the regenerative phenotype are in place in sensory neurons of diabetic rats, but the final commitment, involving the production of GAPs, is impaired. This final point is of importance because studies on the ultrastructure of DRG from diabetic patients show the occurrence of axonal dystrophy, and one possible cause of such a process is intraganglionic sprouting by small nociceptive neurons, which may be triggered by abortive or spasmodic attempts by sensory neurons to regenerate (54). The study by Schmidt et al. (54) demonstrates that abnormal neurofilament accumulations and/or phosphorylation do occur in patients, although the pathology does not include aberrant neurofilament phosphorylation within perikarya. Clearly, this latter point conflicts with the animal model data; however, the perikaryal phenomenon may be transient in diabetes, and this is something that will require testing in the future. Another etiological factor that may induce axonal dystrophy in human DRG is an impairment, or imbalance, in axonal transport (54). Phosphorylation of neurofilament is believed to regulate the incorporation of slow transported neurofilament proteins into the stable cytoskeletal network of the axon and, in turn, modulate axonal caliber (6,55,56). Therefore, aberrant neurofilament phosphorylation within the sensory neuron perikarya and/or axon will result in a malfunction of these processes. This would result in improper ratios and/or spacing between neurofilament species within the axon with a subsequent loss of axonal diameter and integrity, which is observed in animal models of diabetes (1,2).

A reduction in axon diameter, subsequent to neurofilament disturbance, may explain the remarkable change in sural nerve conduction velocity in the 12-week STZ-induced diabetic rats. This reduction, which was almost 50%, is much greater

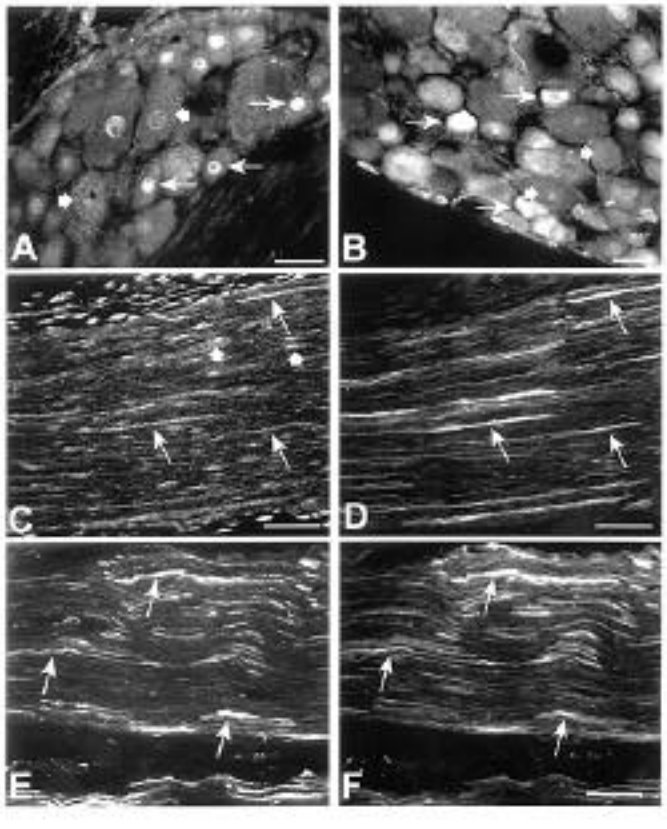

FIG. 4. Localization of JNK in DRG and sciatic nerve. Control tissues of lumbar DRG were probed for total JNK (*A*) and phospho-JNK (*B*). Arrows indicate cells with strong labeling, and the arrowheads show cells exhibiting weaker labeling. Note in *A*, some cells show characteristic granular staining of the cytoplasm. Sciatic nerve was double labeled for total JNK (*C*), synaptophysin (*D*), phospho-JNK (*E*), and synpatophysin (*F*). Arrows show areas of colocalization representing axonal expression of JNK. Arrowheads indicate sites of staining with no colocalization, due to JNK expression by Schwann cells. Scale bars = 25 μm (*A* and *B*) or 100 μm (*C–F*).

TABLE 4
Analysis of neurofilament and JNK phosphorylation in DRG of BB rats

	n	p54 JNK-P (P/Total)	NFM-P (SMI-31)	NFH-P (SMI-31)	NFH-NP (SMI-32)
Control rats	4	1.0 ± 0.58*	1.0 ± 0.1*	1.0 ± 0.06	1.0 ± 0.28
BB rats	6	2.24 ± 0.81†	1.81 ± 0.2†	0.97 ± 0.06	1.12 ± 0.12

Data are means ± SD. BB rats were diabetic for 10–12 months and are compared with weight-matched normal rats. JNK values were derived from 54-kd phosphorylated species, adjusted for total JNK levels, expressed as P/Total, and normalized to control values. The 56-kDa and 46-kDa species of activated JNK were unchanged. * vs. †, $P < 0.02$ (by Student's t test). Regression analysis: JNK-P vs. NFM-P; $r^2 = 0.67$ ($F < 0.002$, highly significant).

than the usual "metabolic" reduction seen in STZ-induced diabetic rats, when a much longer tract of more proximal nerve (from the sciatic notch to the Achilles' tendon) is used for measurement. Restriction to the sural nerve, where the most profound change in neurofilament phosphorylation was seen, suggests that, at this distal point, sensory axons display conduction deficits of a similar magnitude and possibly similar causation to those seen in neuropathic patients.

Several neurofilament kinases that target KSP motifs on the COOH-terminal tail domain of NFM and NFH have been identified; these include JNK (29,30), ERK 1 and 2 (19), glycogen synthase kinase-3α, and cyclin-dependent kinase-5 (20–22). This study showed elevated phosphorylation of JNK and ERK in DRG of diabetic rats, with the related kinase, p38, not being detectable in DRG or sural nerve of control or diabetic rats. Experiments focused on the role of JNK and revealed localization of expression of JNK in sensory neuron perikarya of normal and diabetic adult rats. Recent studies show that NFH is a substrate for stress-activated JNK in cultured neurons (29,30), emphasizing the importance of the relation between activated JNK and aberrant phosphorylation of neurofilaments. In two animal models of type 1 diabetes, the level of phosphorylation of the 54-kDa isoform of JNK 1, 2, and 3 was increased in lumbar DRG and sural nerve (Fig. 1*D* and Tables 3, 4, and 5). The 56- and 46-kDa isoform groupings were already phosphorylated in normal DRG and not further perturbed by the onset of diabetes. This observation suggests that JNK isoforms have functions within the PNS in addition to signaling in response to stress, as previously suggested for the CNS (26).

Immunoreactivity against phosphorylated and total JNK was present in the cytoplasm and nuclei of sensory neuron perikarya of control and STZ-induced diabetic rats (Fig. 4*A* and *B*). No significant differences were observed in the level of phosphorylated JNK detected between control and diabetic DRG. The high levels of endogenous phosphorylation of the 56- and 46-kDa isoforms of JNK in control DRG may have masked the diabetes-induced appearance of the 54-kDa isoform (as observed on Western blotting) (Fig. 1*D*). Interestingly, there was no evidence of a restricted localization of the phosphorylated forms of JNK to the nucleus. In fact, granular staining for phosphorylated JNK within the perikaryal cytoplasm and localization to axons of sensory neurons was observed (Fig. 4*B*, *E*, and *F*). This contradicts previous studies showing activation of JNK to be linked to nuclear localization (26). There is evidence of colocalization of JNK with kinesin on microtubules in non-neurons (57), and we have preliminary data showing bidirectional fast axonal transport of phosphorylated and total JNK in sciatic nerve (manuscript in preparation). The results suggest that in neurons, activation of JNK may result in substrate phosphorylation outside the nucleus, with neurofilament in the perikarya and axon being an obvious candidate.

Axotomy of sensory neurons results in a perikaryal response highlighted by the phosphorylation of JNK (58), elevated activation and expression of c-Jun (58–60), and, as discussed previously, the slower onset of aberrant neurofilament phosphorylation (47,48,61). The ability of JNK to induce or directly phosphorylate neurofilaments may be a component of the neurodegenerative process (29,30). The diabetes-induced phosphorylation of JNK in lumbar DRG (Tables 3 and 4) and sural nerve (Tables 3 and 5) was coupled with the appearance of molecular markers for sensory neuron neurodegeneration, namely, increased phosphorylation of c-Jun and neurofilament. Elevated phosphorylation of ERK was also observed in DRG, but not in sural nerve, of diabetic

TABLE 5
Neurofilament and JNK phosphorylation in sural and peroneal nerves of BB rats

	n	NFH-NP (SMI-32)	NFH-P (SMI-31)	NFH P/NP	NFM-NP (SMI-32)	NFM-P (SMI-31)	NFM P/NP	p54 JNK-P (P/Total)
Sural								
Control rats	5	1.0 ± 0.26†	1.0 ± 0.16	1.0 ± 0.17†	1.0 ± 0.45†	1.0 ± 0.0.46‡	1.0 ± 0.42‡	1.0 ± 0.74*
BB rats	6	2.04 ± 0.65	1.17 ± 0.16	0.59 ± 0.15	0.43 ± 0.12	2.5 ± 0.28	5.43 ± 1.49	2.88 ± 1.12
Peroneal								
Control rats	5	1.0 ± 0.5	1.0 ± 0.26	1.0 ± 0.22†	ND	1.0 ± 0.09*	ND	1.0 ± 0.71
BB rats	6	1.62 ± 0.5	0.88 ± 0.07	0.54 ± 0.17	ND	1.44 ± 0.35	ND	1.55 ± 1.02

Data are means ± SD. *$P < 0.02$, †$P < 0.01$, ‡$P < 0.001$ (all by Student's t test) for control vs. BB rats. ND, not detectable. Levels of phosphorylated p54 JNK were adjusted for total JNK levels and are expressed as P/Total.

rats, implying an absence of any direct association with neurofilament phosphorylation; however, further studies are required (Table 3). In DRG the phosphorylation of JNK was observed as early as 6 weeks of diabetes, before any significant elevation of c-Jun or neurofilament phosphorylation. This may suggest that the appearance of JNK-related neurodegenerative markers may depend upon activation of JNK above a threshold level. It was also apparent that in STZ-induced diabetic and BB rats, the levels of NFM phosphorylation in DRG and sural nerve were greater than those observed for NFH. In fact, in BB rats there was little effect on NFH phosphorylation. This may suggest that NFM phosphorylation may be more strongly linked to diabetes-induced neurodegenerative events and/or a preferred neurofilament substrate of JNK in sensory neurons. Furthermore, in DRG of BB rats, the elevation in phosphorylation of neurofilament and JNK was lower compared with that in the 12-week STZ-induced diabetic rats. Although the BB rats were diabetic for at least 10 months, there were daily injections of insulin, and as such, hyperglycemia was better controlled in comparison with the STZ-induced diabetic rats. In dorsal root of control and STZ-induced diabetic rats, where activated JNK was below detection levels, there was no diabetes-induced alteration in neurofilament phosphorylation (Table 2). Furthermore, in peroneal nerve of BB rats, where NFM phosphorylation was not enhanced, there was an absence of JNK phosphorylation (Table 5). Finally, in motoneuron cell bodies, where neurofilament phosphorylation was absent in diabetes, immunocytochemistry showed that the levels of phospho-JNK were very low. These observations provide strong correlative evidence that phosphorylation of JNK underlies the subsequent enhanced neurofilament phosphorylation in lumbar DRG and sural nerve.

Given the plethora of kinases that are capable of phosphorylating neurofilament, the probability is high that kinases other than JNK and ERK may contribute to dysfunction and that glycation of neurofilament proteins at the NH_2- and COOH-termini may also regulate polymer formation and possibly control levels of degradation (62). Involvement of hyperglycemia-induced glycation in aberrant perikaryal neurofilament phosphorylation cannot be dismissed (44). Nevertheless, this study provides strong correlative evidence that aberrant neurofilament phosphorylation may be linked to phosphorylation of JNK in sensory perikarya and axons and that these phenomena may be linked to the development of a profound fall in nerve conduction velocity in and development of axonopathy in sensory neurons of diabetic rats.

ACKNOWLEDGMENTS

This work was supported by grants from the Wellcome Trust (P.F., D.R.T.) and the Medical Research Council (J.V.P).

We thank Professor J.M. Polak for the gift of antisera to CGRP, and are grateful to the Biomedical Research Facility at the University of Southampton for the supply of BB rats.

REFERENCES

1. Thomas PK, Tomlinson DR, Dyck PJ, Thomas PK, Griffin JW, Low PA, Poduslo JF (Eds.): Peripheral neuropathy. In *Diabetic and Hypoglycaemic Neuropathy*. 3rd ed. Philadelphia, W.B. Saunders, 1992, p. 1219–1250
2. Yagihashi S: Nerve structural defects in diabetic neuropathy: do animals exhibit similar changes? *Neurosci Res Commun* 21:25–32, 1997
3. Jakobsen J: Axonal dwindling in early experimental diabetes. I. A study of cross-sectioned fibres. *Diabetologia* 12:539–546, 1976
4. Yagihashi S, Kamijo M, Ido Y, Mirrlees DJ: Effects of long-term aldose reductase inhibition on development of experimental diabetic neuropathy: ultrastructural and morphometric studies of sural nerve in streptozocin-induced diabetic rats. *Diabetes* 39:690–696, 1990
5. Hoffman PN, Cleveland DW, Griffin JW, Landes PW, Cowan NJ, Price DL: Neurofilament gene expression: a major determinant of axonal caliber. *Proc Natl Acad Sci U S A* 84:3472–3476, 1987
6. De Waegh SM, Lee VM-Y, Brady ST: Local modulation of neurofilament phosphorylation, axonal caliber, and slow axonal transport by myelinating Schwann cells. *Cell* 68:451–463, 1992
7. Hsieh ST, Kidd GJ, Crawford TO, Xu Z, Lin WM, Trapp BD, Cleveland DW, Griffin JW: Regional modulation of neurofilament organization by myelination in normal axons. *J Neurosci* 14:6392–6401, 1994
8. Mohiuddin L, Fernyhough P, Tomlinson DR: Reduced levels of mRNA encoding endoskeletal and growth-associated proteins in sensory ganglia in experimental diabetes mellitus. *Diabetes* 44:25–30, 1995
9. Medori R, Jenich H, Autilio-Gambetti L, Gambetti P: Experimental diabetic neuropathy: similar changes of slow axonal transport and axonal size in different animal models. *J Neurosci* 8:1814–1821, 1988
10. Yagihashi S, Kamijo M, Watanabe K: Reduced myelinated fiber size correlates with loss of axonal neurofilaments in peripheral nerve of chronically streptozotocin diabetic rats. *Am J Pathol* 136:1365–1373, 1990
11. Pekiner C, McLean WG: Neurofilament protein phosphorylation in spinal cord of experimentally diabetic rats. *J Neurochem* 56:1362–1367, 1991
12. Terada M, Yasuda H, Kikkawa R: Delayed Wallerian degeneration and increased neurofilament phosphorylation in sciatic nerves of rats with streptozocin-induced diabetes. *J Neurol Sci* 155:23–30, 1998
13. Gao W-Q, Dybdal N, Shinsky N, Murnane A, Schmelzer C, Siegel M, Keller G, Hefti F, Phillips HS, Winslow JW: Neurotrophin-3 reverses experimental cisplatin-induced peripheral sensory neuropathy. *Ann Neurol* 38:30–37, 1995
14. Gold BG, Price DL, Griffin JW, Rosenfeld J, Hoffman PN, Sternberger NH, Sternberger LA: Neurofilament antigens in acrylamide neuropathy. *J Neuropathol Exp Neurol* 47:145–157, 1988
15. Gold BG, Austin DR: Regulation of aberrant neurofilament phosphorylation in neuronal perikarya. III. Alterations following single and continuous β, β′-iminodipropionitrile administrations. *Brain Res* 563:151–162, 1991
16. Brady ST: Motor neurons and neurofilaments in sickness and in health. *Cell* 73:1–3, 1993
17. Pollanen MS, Bergeron C, Weyer L: Characterization of a shared epitope in cortical Lewy body fibrils and Alzheimer paried helical filaments. *Acta Neuropathol* 88:1–6, 1994
18. Nixon RA: The regulation of neurofilament protein dynamics by phosphorylation: clues to neurofibrillary pathobiology. *Brain Pathol* 3:29–38, 1993
19. Veeranna, Amin ND, Ahn NG, Jaffe H, Winters CA, Grant P, Pant HC: Mitogen-activated protein kinases (Erk 1,2) phosphorylate Lys-Ser-Pro (KSP) repeats in neurofilament proteins NF-H and NF-M. *J Neurosci* 18:4008–4021, 1998
20. Bajaj NPS, Miller CCJ: Phosphorylation of neurofilament heavy-chain side-arm fragments by cyclin-dependent kinase-5 and glycogen synthase kinase-3α in transfected cells. *J Neurochem* 69:737–743, 1997
21. Guidato S, Tsai LH, Woodgett J, Miller CC: Differential cellular phosphorylation of neurofilament heavy side-arms by glycogen synthase kinase-3 and cyclin-dependent kinase-5. *J Neurochem* 66:1698–1706, 1996
22. Shetty KT, Link WT, Pant HC: cdc-2-like kinase from rat spinal cord specifically phosphorylates KSPXK motifs in neurofilament proteins: isolation and characterization. *Proc Natl Acad Sci U S A* 90:6844–6848, 1993
23. Kyriakis JM, Banerjee P, Nikolakaki E, Dai T, Rubie EA, Ahmad MF, Avruch J, Woodgett JR: The stress-activated protein kinase subfamily of c-Jun kinases. *Nature* 369:156–160, 1994
24. Whitmarsh AJ, Davis RJ: Transcription factor AP-1 regulation by mitogen-activated protein kinase signal transduction pathways. *J Mol Med* 74:589–607, 1996
25. Carletti R, Tacconi S, Bettini E, Ferraguti F: Stress-activated protein kinases, a novel family of mitogen-activated protein kinases, are heterogeneously expressed in the adult rat brain and differentially distributed from extracellular-signal-regulated protein kinases. *Neuroscience* 69:1103–1110, 1995
26. Xu X, Raber J, Yang D, Su B, Mucke L: Dynamic regulation of c-Jun N-terminal kinase activity in mouse brain by environmental stimuli. *Proc Natl Acad Sci U S A* 94:12655–12660, 1997
27. Deshmukh M, Johnson EM Jr: Programmed cell death in neurons: focus on the pathway of nerve growth factor deprivation–induced death of sympathetic neurons. *Mol Pharmacol* 51:897–906, 1997
28. Xia Z, Dickens M, Raingeaud J, Davis RJ, Greenberg ME: Opposing effects of ERK and JNK-p38 MAP kinases on apoptosis. *Science* 270:1326–1331, 1995
29. Giasson BI, Mushynski WE: Aberrant stress-induced phosphorylation of perikaryal neurofilaments. *J Biol Chem* 271:30404–30409, 1996
30. Giasson BI, Mushynski WE: Study of proline-directed protein kinases

involved in phosphorylation of the heavy neurofilament subunit. *J Neurosci* 17:9466–9472, 1997
31. Stevens EJ, Carrington AL, Tomlinson DR: Nerve ischaemia in diabetic rats: time-course of development, effect of insulin treatment, plus comparison of streptozotocin and BB models. *Diabetologia* 37:43–48, 1994
32. Filliatreau G, Denoulet P, De Nechaud B, Di Giamberardino L: Stable and metastable cytoskeletal polymers carried by slow axonal transport. *J Neurosci* 8:2227–2233, 1988
33. Cork LC, Sternberger NH, Sternberger LA, Casanova MF, Struble RG, Price DL: Phosphorylated neurofilament antigens in neurofibrillary tangles in Alzheimer's disease. *J Neuropathol Exp Neurol* 45:56–64, 1986
34. Priestley JV, Bachelard H, Turner A (Eds): Immunocytochemical techniques for the study of the nervous system. In *Neurochemistry: A Practical Approach*. 2nd ed. Oxford, Oxford University Press, p. 71–120, 1997
35. Lee VM, Carden MJ, Schlaepfer WW, Trojanowski JQ: Monoclonal antibodies distinguish several differentially phosphorylated states of the two largest rat neurofilament subunits (NF-H and NF-M) and demonstrate their existence in the normal nervous system of adult rats. *J Neurosci* 7:3474–3488, 1987
36. Michael GJ, Averill S, Nitkunan A, Rattray M, Bennett DLH, Yan Q, Priestley JV: Nerve growth factor treatment increases brain-derived neurotrophic factor selectively in TrkA-expressing dorsal root ganglion cells and in their central terminations within the spinal cord. *J Neurosci* 17:8476–8490, 1997
37. Gupta S, Barrett T, Whitmarsh AJ, Cavanagh J, Sluss HK, Derijard B, Davis RJ: Selective interaction of JNK protein kinase isoforms with transcription factors. *EMBO J* 15:2760–2770, 1996
38. Greene DA, Sima AAF, Pfeifer MA, Albers JW: Diabetic neuropathy. *Annu Rev Med* 41:303–317, 1990
39. Greene DA, Stevens MJ, Feldman EL, Thomas TP: The DCCT, metabolism, and diabetic neuropathy: perspectives for the 4th International Symposium on Diabetic Neuropathy. *Neurosci Res Commun* 21:1–4, 1997
40. Diabetes Control and Complications Trial Research Group: The effect of intensive treatment of diabetes on the development and progression of long-term complications in insulin-dependent diabetes mellitus. *N Engl J Med* 329:977–986, 1993
41. Stevens MJ, Dananberg J, Feldman EL, Lattimer SA, Kamijo M, Thomas TP, Shindo H, Sima AAF, Greene DA: The linked roles of nitric oxide, aldose reductase, and (Na^+,K^+)-ATPase in the slowing of nerve conduction in the streptozotocin diabetic rat. *J Clin Invest* 94:853–859, 1994
42. Stevens MJ, Feldman EL, Greene DA: The aetiology of diabetic neuropathy: the combined roles of metabolic and vascular defects. *Diabet Med* 12:566–579, 1995
43. Van Dam PS, Bravenboer B: Oxidative stress and antioxidant treatment in diabetic neuropathy. *Neurosci Res Commun* 21:41–48, 1997
44. Brownlee M: Lilly Lecture 1993. Glycation and diabetic complications. *Diabetes* 43:836–841, 1994
45. Brewster WJ, Fernyhough P, Diemel LT, Mohiuddin L, Tomlinson DR: Diabetic neuropathy, nerve growth factor, and other neurotrophic factors. *Trends Neurosci* 17:321–325, 1994
46. Tomlinson DR, Fernyhough P, Diemel LT: Role of neurotrophins in diabetic neuropathy and treatment with nerve growth factors. *Diabetes* 46:S43–S49, 1997
47. Goldstein ME, Cooper HS, Bruce J, Carden MJ, Lee VM, Schlaepfer WW: Phosphorylation of neurofilament proteins and chromatolysis following transection of rat sciatic nerve. *J Neurosci* 7:1586–1594, 1987
48. Gold BG, Storm-Dickerson T, Austin DR: Regulation of aberrant neurofilament phosphorylation in neuronal perikarya. IV. Evidence for the involvement of two signals. *Brain Res* 626:23–30, 1993
49. Gold BG, Austin DR: Regulation of aberrant neurofilament phosphorylation in neuronal perikarya. I. Production following colchicine application to the sciatic nerve. *J Neuropathol Exp Neurol* 50:615–626, 1991
50. Wong J, Oblinger MM: NGF rescues substance P expression but not neurofilament or tubulin gene expression in axotomized sensory neurons. *J Neurosci* 11:543–552, 1991
51. Fernyhough P, Diemel LT, Brewster WJ, Tomlinson DR: Altered neurotrophin mRNA in peripheral nerve and skeletal muscle of experimentally diabetic rats. *J Neurochem* 64:1231–1237, 1995
52. Sebert ME, Shooter EM: Expression of mRNA for neurotrophic factors and their receptors in the rat dorsal root ganglion and sciatic nerve following nerve injury. *J Neurosci Res* 36:357–367, 1993
53. Skene JH: Axonal growth-associated proteins [review; 155 references]. *Annu Rev Neurosci* 12:127–156, 1989
54. Schmidt RE, Dorsey D, Parvin CA, Beaudet LN, Plurad SB, Roth KA: Dystrophic axonal swellings develop as a function of age and diabetes in human dorsal root ganglia. *J Neuropathol Exp Neurol* 56:1028–1043, 1997
55. Lewis SE, Nixon RA: Multiple phosphorylated variants of the high molecular mass subunit of neurofilaments in axons of retinal cell neurons: characterization and evidence for their differential association with stationary and moving neurofilaments. *J Cell Biol* 107:2689–2701, 1988
56. Archer DR, Watson DF, Griffin JW: Phosphorylation-dependent immunoreactivity of neurofilaments and the rate of slow axonal transport in the central and peripheral axons of the rat dorsal root ganglion. *J Neurochem* 62:1119–1125, 1994
57. Nagata K, Puls A, Futter G, Aspenstrom P, Schaefer E, Nakata T, Hirokawa N, Hall A: The MAP kinase kinase kinase MLK2 colocalizes with activated JNK along microtubules and associates with kinesin superfamily motor KIF3. *EMBO J* 17:149–158, 1998
58. Kenney AM, Kocsis JD: Peripheral axotomy induces long-term c-Jun amino-terminal kinase-1 activation and activator protein-1 binding activity by c-Jun and junD in adult rat dorsal root ganglia in vivo. *J Neurosci* 18:1318–1328, 1998
59. Jenkins R, McMahon SB, Bond AB, Hunt SP: Expression of c-Jun as a response to dorsal root and peripheral nerve section in damaged and adjacent intact primary sensory neurons in the rat. *Eur J Neurosci* 5:751–759, 1993
60. Gold BG, Austin DR, Storm-Dickerson T: Multiple signals underlie the axotomy-induced upregulation of c-JUN in adult sensory neurons. *Neurosci Lett* 176:123–127, 1994
61. Gold BG, Austin DR, Griffin JW: Regulation of aberrant neurofilament phosphorylation in neuronal perikarya. II. Correlation with continued axonal elongation following axotomy. *J Neuropathol Exp Neurol* 50:627–648, 1991
62. Dong DL-Y, Xu Z-S, Chevrier MR, Cotter RJ, Cleveland DW, Hart GW: Glycosylation of mammalian neurofilaments: localization of multiple *O*-linked *N*-acetylglucosamine moieties on neurofilament polypeptides L and M. *J Biol Chem* 268:16679–16687, 1993